

Analysis and Efficient Onset Time Detection of Acoustic Emission Signals with Power Constrained Sensor Platforms

Benjamin Babjak, Sandor Szilvasi, Peter Volgyesi
Institute for Software Integrated Systems,
Department of Electrical Engineering and Computer Science,
Vanderbilt University, Nashville, Tennessee
Email: {benjamin.babjak, sandor.szilvasi, peter.volgyesi}@vanderbilt.edu

Ozgur Yapar, Prodyot K. Basu
Department of Civil & Environmental Engineering,
Vanderbilt University, Nashville, Tennessee
Email: {ozgur.yapar, p.k.basu}@vanderbilt.edu

Abstract— In this paper we describe our custom designed, low-power, intelligent sensor platform, and a novel analysis approach for Structural Health Monitoring (SHM). More specifically we show how Acoustic Emission (AE) signals were recorded during aluminium and steel beam break tests utilizing two channels on our MarmotE platform, and how subsequent low-resource but accurate onset time detection yielded Time Difference of Arrival (TDoA) results. We also demonstrate a new, simplified method to pick valid AE events from a vast set of noisy measurements, and prove the feasibility of our ideas by showing that our approach provided results comparable to widely used industry methods with modest resource requirements.

I. INTRODUCTION

The goal of SHM is to give insight into the condition and state of structures with emphasis on damage detection. AE-based SHM methods [1] are preferred as on-site, non-destructive approaches, which mainly detect ultrasound stress waves caused by sudden, inner structural changes. The sources of AE signals can be damage-related, but alternative causes are also possible introducing background noise. The nature and location of the damage may be estimated by using one or a combination of measured parameters, such as the TDoA between different transducers. In this paper, we give an overview of our most important results and examine a simple use case example.

The main contributions of this work are i) the development and SHM application of our sensor platform ii) a less resource intensive, accurate onset time detection algorithm, and iii) classification of AE events based on a novel quality index. We evaluate the system using aluminium and steel beam break tests, and show the practicality of wavelet time-frequency analysis to distinguish between valid AE signals originating from various sources.

II. MEASUREMENT PROCEDURE

To determine our system’s capability, two aluminium American Standard 6061-T6 type I-beams and a S3x5.7 section of ASTM A36 steel beam were tested, see Table I. First, the beams were partially sawn in the middle, so that damages would form in a reasonable amount of time at a known location

under a reasonable load. The beams were then mounted to supports on both ends, and an electro-mechanical shaker below the middle of the specimen was connected to the beam center with a tight link that would not impede crack growth. The system of two supports and the shaker-specimen link formed 3-point bending conditions, see Fig. 1. Measurement sessions consisted of several approximately 20 minute long intervals, employing successively increasing shaker amplitudes. Two PKWDI AE microphones were mounted on the beams at different distances from the crack.

TABLE I
DIMENSIONS OF THE TESTED METAL BEAMS.

	Aluminium		Steel
	1st beam	2nd beam	
length [foot]	11	8	11
depth [inch]	3	3	3
width [inch]	2.509	2.509	2.330

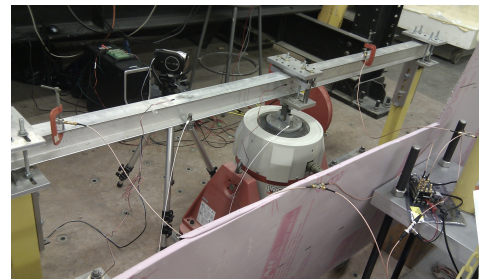


Fig. 1. Aluminium break test setup, with 8 foot long beam.

III. THE MARMOTE SENSOR PLATFORM

We used our custom-designed, universal, low-power, multi-channel, wireless sensor node [2] to detect AE events. The platform can be physically and logically divided into three parts, see Fig. 2. The bottom layer manages the energy supply, featuring power consumption monitoring and interfaces for batteries, wall power, and other sources including energy harvesting units. The middle layer is responsible for domain

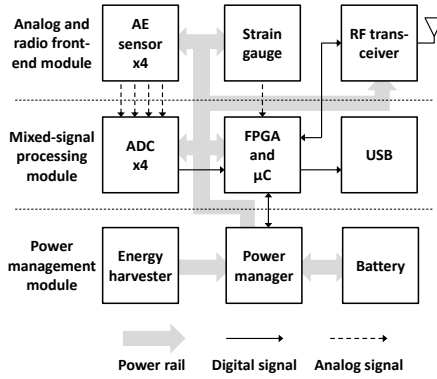


Fig. 2. Simplified block diagram of the MarmotE sensor platform.

conversion, digital processing based on the SmartFusion Flash Field-Programmable Gate Array (FPGA), and high-speed connectivity such as a Universal Serial Bus (USB) or Ethernet. The application-specific front-end layer has baseband amplifiers and carries a Radio Frequency (RF) chip for wireless communication.

IV. ANALYSIS AND PROCESSING

Fig. 3 depicts AE analysis – note that the actual signal processing takes place on the Personal Computer (PC), and the sensor platform is only responsible for streaming raw data. The power supply for the active microphones (not shown) is provided by the power board. Unity gain op-amp circuits convert single-ended inputs to differential outputs. Signals are sampled with 10-bit resolution at a rate of 750 kHz by Analog-to-Digital Converters (ADCs), which connect to the SmartFusion FPGA using a parallel Double Data Rate (DDR) interface. The FPGA has sufficient resources for signal processing, but in our case, it only streamed continuous frames of raw samples to the PC. Signal analysis was developed in Python/NumPy and C++ utilizing the GNU Radio framework.

1) *Valid AE event pre-selection*: Since background noise has significant energy concentrated in the lower frequency ranges, a 15 tap Finite Impulse Response (FIR) High-Pass Filter (HPF) (cutoff frequency 50 kHz, attenuation 50 dB) is employed. From the data stream, the system collects time windows in which the signal crossed the threshold level.

2) *Time-frequency analysis with wavelet transform*: The wavelet transform is a widely-used method for time-frequency analysis and has several advantages over Fourier transform based solutions, one of the most important being its ability to adapt the transform process itself to the examined signal. See Fig. 8 and 9 for a preliminary example for distinguishing between measurements based on their time-frequency signatures.

3) *Event classification and parameter estimation*: Our method for accurate onset time estimates and for separation of valid AE events from false positives was to first provide a short time window around the event, then to calculate a “utility” or “fitness” function that would give a minimum at the exact start of an AE event within the window.

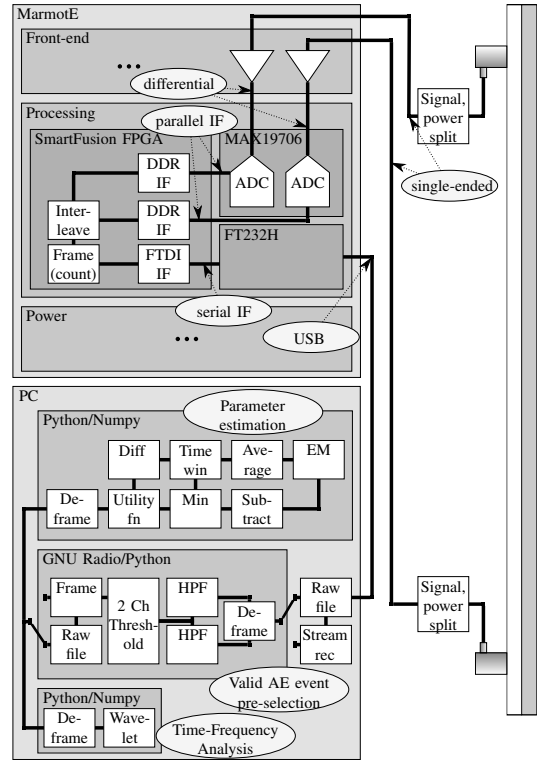


Fig. 3. Simplified block diagram of the AE signal processing.

a) *Utility function 1. - The Akaike’s Information Criterion (AIC)-based onset time selector*: Originally, AIC [3] was meant for statistical model identification, but was later applied to modeling non-stationary, non-overlapping, independent time series with different AutoRegressive (AR) model properties [4]. Because AR model estimation is so resource-consuming, a simpler method was proposed [5], dealing with only two, subsequent time series, see (1).

$$AIC(k) = k \ln \left(\text{var}(x[1, k]) \right) + (N - k - 1) \ln \left(\text{var}(x[k + 1, N]) \right) \quad (1)$$

Where $x[1, k]$ is the time series starting with the first sample and ending with (and inclusive of) the k th, N is the number of samples, and $\text{var}() = \frac{1}{N-1} \sum_{i=1}^N (x_i - \bar{x}_i)^2 = \widehat{\sigma}_2^2$ is a variance estimate. Variations on the calculation of $\text{var}()$ can be found in literature. The k value giving the minimum $AIC(k)$ is the most likely onset time index.

It can be mathematically proven that if both time series have constant but different variances (which holds e.g. for Gaussian white noise), the method will point to the onset time of the second series. However, the crucial realization here is that the original AIC method’s variance was AR estimation error related, while this latter method is a direct variance of a signal part; thus (without a DC component), the approach boils down to a simple comparison of signal energy in two parts of the time window. Note that for Gaussian white noise, the variance is equal to half of the noise spectral density: $\sigma^2 = \frac{N_0}{2}$.

b) *Utility function 2.* - *The reciprocal-based onset time selector:* We examined several other utility functions that achieve similar performance to AIC but are significantly simpler. A reciprocal relationship, as seen in (2), stood out in particular.

$$\text{fitness function} = -\frac{n_1}{\sigma_1^2} - \frac{n_2}{\sigma_2^2} \quad (2)$$

Where n_1 is the length of the first time series, n_2 is the length of the second, σ_1^2 is the variance estimate of the first block, σ_2^2 is the same for the second.

The advantages are i) no logarithm calculation, and ii) better onset time estimates for some signals (mathematically proven). Experience showed that dispersive signals were handled better, and empirical evidence also suggests that in most cases $-\frac{n_1}{\sigma_1^2}$ is a sufficient approximation of the fitness function.

c) *Quality index for measurements:* To distinguish AE events from noise events, signal energy-based methods are often times suggested in the literature, but these approaches are usually unreliable; thus, we devised a different “quality index” indicator. Recall that onset time is the point where the fitness function reaches its minimum. The quality of the measurement is then estimated with (3).

$$q = \frac{1}{M} \sum_{i=i_{min}}^{i_{min}+M} (g_i - g_{i-1}) \quad (3)$$

Where q is the quality index, g is the utility function, M is the sample number, and i_{min} is the fitness function minimum index. The idea stems from the observation that for valid measurements, utility functions decrease rapidly towards the minimum, then steeply increase, whereas for noise, no such trend is noticeable. Thus, if the fitness function’s derivative is taken, the values after i_{min} tend to be notably higher than zero for real AE events. The quality index is hence the mean of a few (e.g. $M = 40$) derivative values right after i_{min} .

d) *Expectation–Maximization (EM) method:* With all possible AE events at hand, the TDoA of the crack location is estimated. In this context, time difference is a random variable, and as such, statistical tools are employed to estimate its mean value. The AE events form clusters in a two dimensional measurement space (quality index and AE) where the number of random processes – that is the number of AE sources – is unknown. We assume a Gaussian Mixture Model (GMM) with at least two mixed independent processes (i.e. the noisy events and valid AE events). No closed formulas exist to estimate a multi-dimensional GMM’s parameters, so we utilize the EM algorithm instead, which iteratively converges to the Maximum Likelihood (ML) estimate. A disadvantage is that this method easily finds local maxima and is very sensitive to numerical representation.

V. SUMMARY OF RESULTS

Fig. 4 and 5 show the AIC- and reciprocal-based onset time selectors respectively, with the latter seeming to give an overly

early onset time estimate. Proper magnification reveals that the first signal components have indeed arrived at that time, so it has actually provided a better estimate in this case.

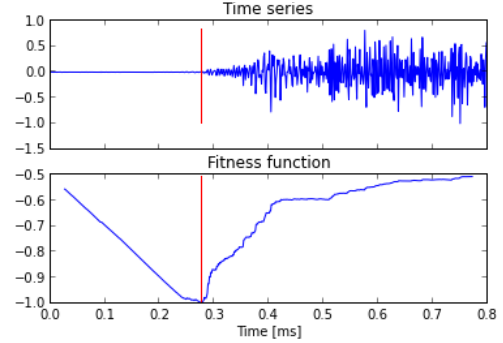


Fig. 4. AIC-based result; red vertical line marks the onset time as detected.

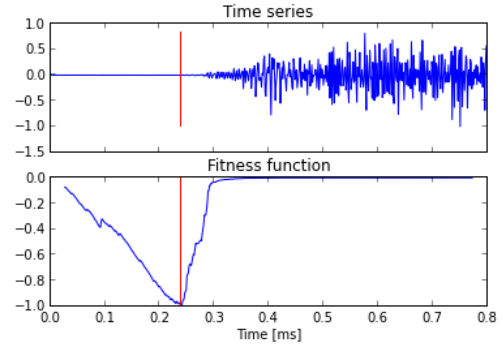


Fig. 5. Reciprocal selector result; red vertical line marks the onset time as detected.

Fig. 6 and 7 show the results of our EM event grouping and parameter estimation for the first aluminium test. Looking at the AIC results, the events with a log quality index of -3.5 at around 0.2 ms stem from the break in the beam, points below -4 can be considered useless noise events, and a third cluster unexpectedly appeared as well with high quality indices at 0.8 ms. Closer inspection revealed that it was not caused by reflected waves, but very likely originated from outside the beam (i.e. the supports). Because of the quite different TDoAs, it was simple to categorize the measurements, and a look at their Wavelet Packet Decomposition (WPD), see Fig. 8 and 9, revealed fundamental differences in energy distribution in the time-frequency domain confirming the different origins.

TABLE II

THE STEEL BREAK TEST CRACK LOCATION ESTIMATES FOR TWO ONSET TIME PICKERS. ACTUAL CRACK LOCATION AT -78.7 cm.

shaker amplitude [inch]	onset time detection	log quality index	time difference [ms]	sound speed [$\frac{m}{s}$]	distance difference [cm]
0.15	AIC	-3.84	-0.2134	3549.50	-75.8
	reciprocal	-2.78	-0.1913	4243.36	-81.2
0.2	AIC	-3.74	-0.1972	3549.50	-70.0
	reciprocal	-2.19	-0.1903	4243.36	-80.8

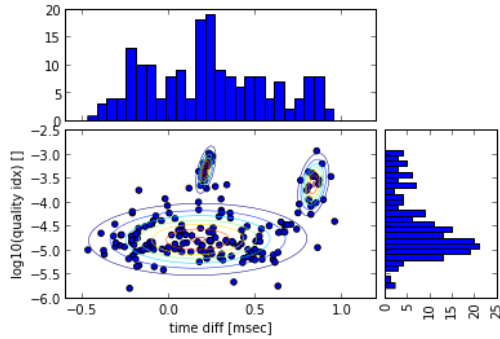


Fig. 6. AIC-based onset time picker results. Gaussian distributions as estimated by the EM algorithm for the first aluminium break test with shaker set to 0.5 inch amplitude.

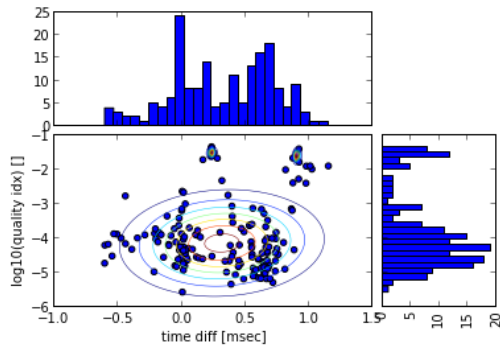


Fig. 7. Reciprocal onset time picker. Gaussian distributions as estimated by the EM algorithm for the first aluminium break test with shaker set to 0.5 inch amplitude.

Given the simple, one dimensional measurement setup, an accordingly uncomplicated damage localization approach was utilized. The above described onset time selecting methods gave TDoAs, which, in conjunction with accurate sound propagation speed estimates, yielded damage location information. Sound speed was measured and estimated separately, but using the same framework. In the end, both the AIC and the reciprocal method gave varying damage location errors of around 10-15 cm for the initial aluminium tests. A likely source of error was the fact that sound speed measurements were not performed directly before the break test. For the steel break measurement, the distance difference ground truth was -78.7 cm. The sound speed was measured right before the actual break, which proved very beneficial in reducing the reciprocal onset time detection error to around 2 cm. The AIC-based method benefited from that as well, but still managed to give a worse error of around 9 cm in this case.

VI. CONCLUSION

We have successfully designed and employed a novel sensor platform for recording and distinguishing between AE events. We have demonstrated accurate onset time detection with a simpler method giving comparable results to the prevailing AIC-based approach. We have shown that our quality index calculation is capable of indicating good readings and local-

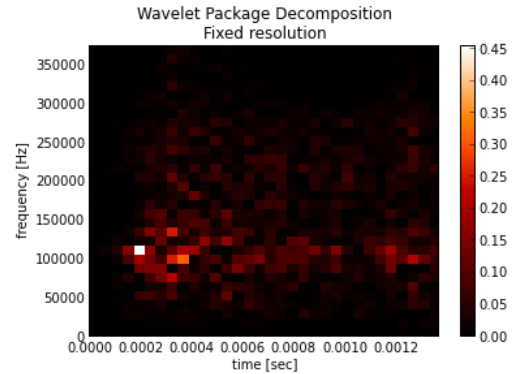


Fig. 8. Time-frequency characteristics of AE events from two different sources at the first aluminium break setup. AE event with time difference of around 0.2 ms.

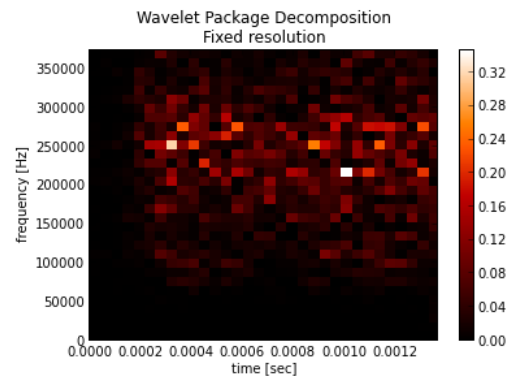


Fig. 9. Time-frequency characteristics of AE events from two different sources at the first aluminium break setup. AE event with time difference of around 0.8 ms.

ization accuracy. Our briefly presented, preliminary results suggest that the algorithms, concepts, and methods developed are feasible, and uniquely applicable to aid more in-depth analysis performed by domain experts.

ACKNOWLEDGMENT

This work was supported by the National Science Foundation awards #0964592 and #1035627.

REFERENCES

- [1] B. Muravin, G. Muravin, and L. Lezvinisky, "The Fundamentals of Structural Health Monitoring By The Acoustic Emission Method," in *20th International Acoustic Emission Symposium*, Kumamoto, pp. 253–258.
- [2] B. Babjak, S. Szilvasi, A. Pedchenko, M. Hofacker, E. J. Barth, P. Volgyesi, and A. Ledeczki, "Experimental Research Platform for Structural Health Monitoring," in *Advancement in Sensing Technology Smart Sensors, Measurement and Instrumentation*. Springer Berlin Heidelberg, 2013, vol. 1, pp. 43–68.
- [3] H. Akaike, "A new look at the statistical model identification," *IEEE Transactions on Automatic Control*, vol. 19, no. 6, pp. 716–723, Dec. 1974.
- [4] G. Kitagawa and H. Akaike, "A procedure for the modeling of non-stationary time series," *Annals of the Institute of Statistical Mathematics*, vol. 30, no. 1, pp. 351–363, Dec. 1978.
- [5] N. Maeda, "A method for reading and checking phase times in auto-processing system of seismic wave data," *Zisin, Journal of the Seismological Society of Japan*, vol. 38, pp. 365–380, 1985.